Turkish Computational and Theoretical Chemistry

Turkish Comp Theo Chem (TC&TC)

Volume(Issue): 1(2) – Year: 2017 – Pages: 13-26

ISSN: 2587-1722 / e-ISSN: 2602-3237

Received: 19.05.2017 **Accepted:** 15.06.2017 *Research Article*

Spectroscopic and Quantum Chemical Studies on Some β-Lactam Inhibitors

Sultan Erkan Kariper[1]

Chemistry and Chemical Process Technology, Yıldızeli Vocational School, Cumhuriyet University, Sivas, Turkey

Abstract: Amoxicillin (Amox) and ampicillin (Amp) are investigated by using quantum mechanical methods. These compounds was confirmed by XRD analysis and optimized bond parameters were calculated by density functional (DFT) at B3LYP/6-31G(d) level. The optimized geometrical parameters are in good agreement with crystal data. The experimentally observed FT-IR and NMR picks were assigned to calculated modes for the molecules. Some molecular descriptors are calculated with density functional theory (DFT/B3LYP) 6-31G(d) level in the gas phase. The highest occupied molecular orbital energy (EHOMO), the lowest unoccupied molecular orbital energy (ELUMO), the energy difference (ΔE), hardness (η), softness (σ), electronegativity (χ), chemical potential (μ), electrophilicity index (ω) and nucleophilicity index (ε) are calculated in the this level and associated with inhibition efficiencies of the mentioned β-lactam inhibitors. Molecular Electrostatic Potential (MEP) maps were investigated and predicted the reactive sites. Some quantum chemical descriptors which are total static dipole moment (μ), the average linear polarizability (α), the anisotropy of the polarizability (Δα) and first hyperpolarizability (β) were evaluated for explaining the NLO properties in studies molecules. The inhibition activities were studied using molecular docking studies. The antibiotics were docked into the cocrystallized structure of PXR with SR12813 (PDB ID: 1NRL). Docking results and order of inhibition activity associated with quantum chemical parameters was the same as that of experimental inhibition activity.

Keywords: *β-lactam, DFT, Molecular Docking, Quantum Chemical Parameters.*

Graphical Abstract

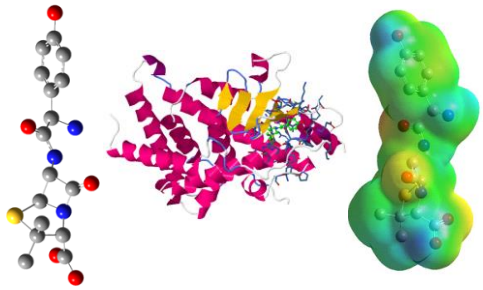

Amoxicillin (Amox) and ampicillin (Amp) were investigated by using quantum mechanical methods. Optimized geometrical parameters, IR and NMR spectroscopic studies were provided for the structure elucidation of chemical species. NLO properties of related molecules are investiggated. Docking was used to predict the bound conformation and binding free energy of small molecules to the target.

[1] Corresponding Author

e-mail: sultanerkan58@gmail.com

1. Introduction

β-lactams have been discovered at the beginning of the twentieth century and they are used in the struggle against pathogenic bacteria [1]. These compounds have the antibacterial effect because they contain amino and carbonyl groups as well as the nitrogen and sulfur atoms in the aromatic structure [2]. In addition, β-lactam antibiotics are applied in the treatment of neurological disorders such as Alzheimer's disease, Parkinson's disease, prion diseases and amyotrophic lateral sclerosis (ALS) [3,4]. Transition metal chelates of β-lactams are effective to prevent the most neurological diseases [5-10].

Amoxicillin (Amox) and ampicillin (Amp) exhibit a similar antibacterial spectrum. Amoxicillin (Amox) and ampicillin (Amp) are two β-lactam antibiotics derivatives. Amox and Amp are effective against both gram-positive and gram-negative organisms which are various pathogenic enteric organisms. Amp is used to infections caused by Escherichia coli, Salmonella, Proteus and Klebsiella [11].

Amox and Amp have not been extensively evaluated in the literature with experimental and theoretical chemistry methods. For this reason, these compounds with vital precautions have been extensively studied, which is spectroscopic behavior and quantum chemical approaches. Density function theory (DFT) is one of the most widely used methods for spectroscopic and quantum chemical studies theoretically in recent years for chemical compounds.

Structural parameters (bond lengths and bond angles) and spectroscopic studies (IR and NMR) provide a basis for the structure elucidation of chemical species. Computational chemistry methods provide visual and detailed analysis of these studies. Non-linear optical (NLO) features have become a very interesting subject due to their potential applications such as optoelectronic devices, optical modulation, molecular switching and optical memory [12]. Therefore, a wide variety of molecular systems inorganic, organic and organometallic were investigated for NLO activity. Some quantum chemical descriptors which are total static dipole moment (μ), the average linear polarizability (α), the anisotropy of the polarizability (Δα) and first hyperpolarizability (β) have been used for explaining the NLO properties in many computational studies. Molecular electrostatic potential (MEP) maps are used to predict the atom with the higher electron density in a molecule. MEP is the potential generated by the charge distribution of a molecule and denotes chemical reactivity, showing nucleophilic and electrophilic sites indicated by MEP maps [13]. For this reason, MEP maps of β-lactam compounds are examined. Molecular descriptors are obtained with quantum chemical calculations. These molecular descriptors are the highest occupied molecular orbital energy (E_{HOMO}), the lowest unoccupied molecular orbital energy (E_{LUMO}), the energy gap (ΔE), hardness (η), softness (σ), electronegativity (χ), chemical potential (μ), electrophilicity index (ω) and nucleophilicity index (ε). Computational docking programs examine interactions with a chemical compound and are widely used for drug discovery and development. Docking is used to predicting the bound conformation and binding free energy of small molecules to the target. Docking Server is a free open source software package for virtual placement of small molecules into macromolecular receptors and developed for making related accounts.

In this study, the studied compounds are optimized at DFT/B3LYP/6-31G(d) level both in the gas phase. The structural parameters are examined and compared with the data obtained from X-rays for Amox and Amp. The computed and experimentally observed spectroscopic values are examined on the β-lactams to give a detailed assignment of the fundamental bands in FT-IR and NMR. The chemical activity areas of the studied compounds are determined via MEP maps. The quantum chemical identifiers are associated with the activities of the compounds. NLO materials have been calculated due to promising applications in optoelectronic technology. For the compounds with the target protein are reviewed to the interacting energies by Molecular Docking studies and are determined to the interaction types and interaction regions.

2. Computational Details

The investigated compounds were drawn with the Gauss View 5.0.8 package program for molecular geometry optimization [14] and the calculation was performed via Gaussian 09 Revision C.01 programme pack (Linux based) in

TÜBİTAK-TR Grid [15]. The calculations included Density Functional Theory (DFT) hybrid B3LYP [16] and used to 6-31G (d) basic sets. Molecular geometries were optimized using B3LYP/6-31G (d) level in the gas phase. IR spectrum was obtained from optimized structures and the frequencies obtained as harmonic were converted to anharmonic frequencies with a scale factor of 0.9600 [17].The proton and carbon NMR chemical shift was calculated with the gauge-including atomic orbital (GIAO) approach by using B3LYP/6-31G(d) level of the studied molecule. Molecular docking (ligand-protein) simulations were performed by using DockingServer free software package.

The total static dipole moment (μ), the mean polarizability (α), the anisotropy of the polarizability (Δα) and the total static first hyperpolarizability (β) using x, y, z components are defined as using Eqs. 1-4 [18].

$$\mu = \left(\mu_x^{\,2} + \mu_y^{\,2} + \mu_z^{\,2}\right)^{1/2} \quad (1)$$

$$a = \frac{1}{3}\left(a_{xx} + a_{yy} + a_{zz}\right) \quad (2)$$

$$\Delta a = \frac{1}{\sqrt{2}}\left[\begin{array}{l}\left(a_{xx} - a_{yy}\right)^2 + \left(a_{yy} - a_{zz}\right)^2 + \\ \left(a_{zz} - a_{xx}\right)^2 + 6a_{xz}^{\,2} + 6a_{xy}^{\,2} + 6a_{yz}^{\,2}\end{array}\right]^{1/2} \quad (3)$$

$$\Delta a = \frac{1}{\sqrt{2}}\left[\begin{array}{l}\left(a_{xx} - a_{yy}\right)^2 + \left(a_{yy} - a_{zz}\right)^2 + \\ \left(a_{zz} - a_{xx}\right)^2 + 6a_{xz}^{\,2} + 6a_{xy}^{\,2} + 6a_{yz}^{\,2}\end{array}\right]^{1/2} \quad (4)$$

According the Koopman's theorem, as can be seen from eq. (5)-(6), Elumo and EHOMO of any chemical species have been associated with its ionization energy and electron affinity values [19-22]

$$I = -E_{HOMO} \quad (5)$$

$$A = -E_{LUMO} \quad (6)$$

Energy gap (ΔE) [23], absolute electronegativity (χ), chemical potential (μ), absolute hardness (η) and absolute softness (σ) are given by eq. (7-11) [24].

$$\Delta E = E_{LUMO} - E_{HOMO} \quad (7)$$

$$\chi = \frac{I+A}{2} \quad (8)$$

$$\mu = -\chi \quad (9)$$

$$\eta = \frac{I-A}{2} \quad (10)$$

$$\sigma = \frac{1}{\eta} \quad (11)$$

Parr et al. have defined electrophilicty index as a measure of energy lowering due to maximal electro flow between donor and acceptor [25].

$$\omega = \frac{\mu^2}{2\eta} \quad (12)$$

Kiyooka et al. have detected that the ω is a function of μ/η in the second-order parabola for various species [26] and they have proposed the ε parameter related to nucleophilicty index.

$$\varepsilon = \mu\eta \quad (13)$$

3. Results and discussion

3.1. Optimized Geometry

The optimized structures of Amox and Amp are shown Figure 1 and the structure parameters (bond length and bond angles) are listed in Table 1 using DFT/B3LYP/6-31G(d) level in the gas phase. The calculated bond lengths are compared with X-ray diffraction data [27]. It can be seen that the results obtained with the calculated values are in agreement with the crystallographic data.

The bond lengths (S-C1, S-C3, C1-C2, C2-N1, N1-C3, N1-C5, C3-C4, C4-C5 and C5-O1) of the Amox and Amp are correlated with X-ray data and R2 values are determined as 0.9756 and 0.9930, respectively. It is shown that the correlation coefficients (R2) close to 1 which provide remarkable data of the theoretical calculations. Therefore, bond lengths which are not in the literature can be foreseen.

Frau et al. investigated the C1-S-C3, C3-N1-C5, O1-C5-N1, C3-N1-C2, C5-N1-C2, C4-C5-N1 and C5-C4-C3 bonds for Amox and compared them with X-ray data. They are given in Table 2 and compared the calculated bond angles with X-ray data.

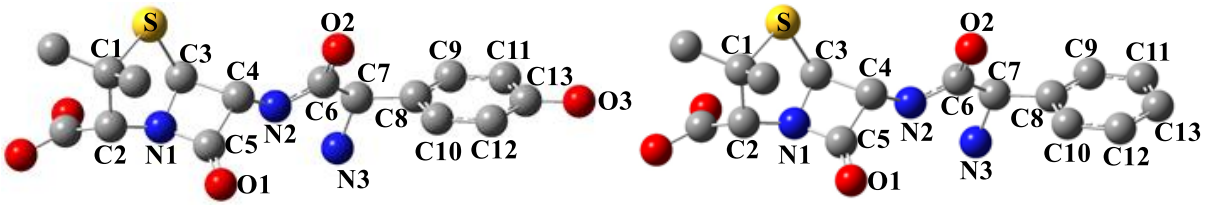

Figure 1. Optimized structure and numbering of Amox and Amp. Hydrogen atoms are not presented for clarity.

Table 1. The calculated and X-ray bond lengths of Amox and Amp

	Amox		Amp	
Bond length	Calc.	X-ray	Calc.	X-ray
S-C1	1.880	1.843	1.881	1.850
S-C3	1.850	1.775	1.851	1.810
C1-C2	1.584	1.559	1.584	1.550
C2-N1	1.443	1.456	1.443	1.460
N1-C3	1.462	1.492	1.462	1.450
N1-C5	1.398	1.381	1.399	1.380
C3-C4	1.571	1.575	1.571	1.530
C4-C5	1.556	1.515	1.556	1.520
C5-O1	1.206	1.200	1.206	1.180
C4-N2	1.427	-	1.427	-
N2-C6	1.369	-	1.369	-
C6-O2	1.222	-	1.222	-
C6-C7	1.547	-	1.546	-
C7-N3	1.546	-	1.481	-
C7-C8	1.518	-	1.521	-
C8-C9	1.401	-	1.399	-
C8-C10	1.401	-	1.402	-
C9-C11	1.392	-	1.396	-
C10-C12	1.393	-	1.394	-
C12-C13	1.399	-	1.397	-
C13-O3	1.367	-	-	-

Table 2. The calculated and X-ray bond angles of Amox and Amp

		Amox	Amp.
Bond angles	Calc.	X-ray	Calc.
C1-S-C3	94.3	90.1	94.3
C3-N1-C5	94.9	93.3	94.9
O1-C5-N1	131.3	131.2	131.3
C3-N1-C2	117.9	117.1	117.9
C5-N1-C2	128.6	127.5	128.6
C4-C5-N1	91.4	93.0	91.4
C5-C4-C3	84.7	85.1	84.8

As a result, R2 value is calculated as 0.991 for Amox. Additionally, bond angles of Amp are given in Table 2, too. The graphs are plotted for Amox and Amp both bond length and bond angle and given in supplementary material. (Supp. Fig. S1). As shown in Table 2, there is a deviation from the ideal geometry at the bond angles of the lactam ring where is the square part and the sulfur ring of the mentioned molecules above. For example, C3-N1-C5, C4-C5-N1 and C5-C4-C3 angles are found as 94.9, 91.4 and 84.7, respectively.

3.2. IR Analysis

A band may consist of multiple vibrational transition in the IR spectrum. Some of the vibrational transitions that form a band are violent and some are weak. Some of the vibrational transitions that form a band are violent and some are weak. Vibrational transition with high severity makes more contribution to band [28]. For this reason, in this study, vibrational transition frequency with the highest intensity in a band was given and all the vibrational movements that make up the band are labeled. The frequencies obtained after the optimization of the molecules are harmonic frequencies and the frequencies obtained experimentally are also anharmonic frequencies. Gaussian calculations provide a scale factor which is converted harmonic frequencies into anharmonic frequencies. The scale factor is 0.9600 of B3LYP method and 6-31G(d) basic set [29]. The vibrational spectra obtained from the optimized structures which calculated at B3LYP/6-31G(d) level in the gas phase of Amox and Amp were given in Figure 2.

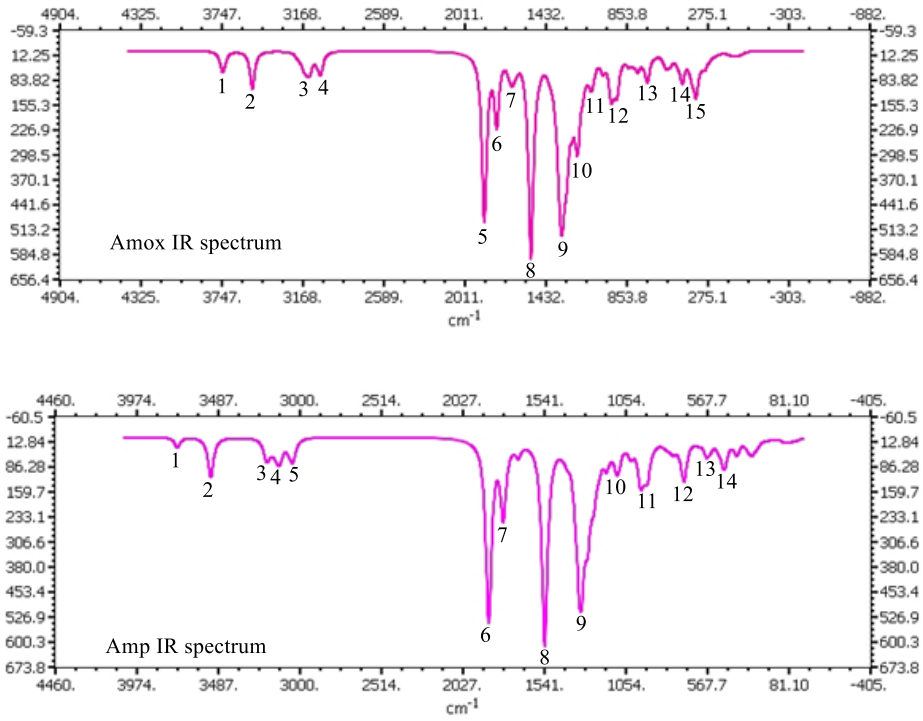

Figure 2. IR spectra of Amox and Amp

As seen in Figure 2, 15 peaks for Amox and 14 peaks for Amp were labeled. Table 3 indicates the anharmonic frequencies for Amox and Amp and the detailed labeling of these vibration modes with obtained at B3LYP/6-31G(d) in the gas phase. According to Table 3, the bond vibrational frequency of the specific OH group of Amox is 3600.1 cm^{-1}. This value in the literature is 3552 cm-1. The N-H vibrational frequency calculated for Amox is 3392.5 cm^{-1} and the experimental frequency is 3161 cm^{-1}. C = O frequency experimentally measured in the β-lactam and amide

region is labeled as 1775 and 1686 cm-1 and the calculated frequencies are found as 1800.7 and 1717.1 cm^{-1}, respectively. Although the experimental value of the N-H bending stretching frequency is 1560 cm^{-1}, the calculated value is determined as 1717.1 and 1481.4 cm^{-1} by an animation program. Observation of other vibrational types besides N-H bending stretching may cause a certain difference between experimental and calculated. The CN bond stretching frequency in the square part is calculated as 1069.9 cm^{-1}, the experimental value of this stretching is 1021 cm^{-1}. The calculated frequency for CS bond stretching is 554.9 cm^{-1} while the experimental stretching is 582 cm^{-1}.

The experimental vibrational frequencies of N-H, C=O of β-lactam and amide region, N-H bending stretching, CN and CS in the Amp are 3200, 1774, 1688, 1516, 1075 and 598 cm^{-1}, respectively. The calculated values for these stretching types are also 3395.1, 1880.8, 1718.8, 1481.6, 1284.4 and 555.6 cm^{-1}. The theoretical and experimental results for some stretching frequencies are very close to each other. Vibration spectroscopy is an effective tool for illuminating the molecular structure and gives a dynamic image of the molecule [30]. The used method and the basic set are chosen quite appropriately for structure verification.

Table 3. Calculated anharmonik frequencies (cm^{-1}) and assignments for Amox and Amp.

	Amox		Amp	
	Anhar. IR	Assign.	Anhar. IR	Assign.
1	3600.1	STRE O-H	3587.3	STRE COO-H
2	3392.5	STRE N-H	3395.1	STRE N-H
3	3005.5	STRE C-H	3072.1	STRE C-H(aro.)
4	2928.1	STRE CH_3	3004.2	STRE C-H
5	1800.7	STRE C=O	2928.5	STRE CH3
6	1717.1	STRE C=O BEND N-H	1800.8	STRE C=O
7	1609.5	STRE C-C(aro.)	1718.8	STRE C=O BEND N-H
8	1481.4	STRE C-N BEND N-H	1481.6	STRE C-N BEND N-H
9	1284.1	STRE C-N BEND C-H	1284.4	STRE C-N (square part) BEND C-H
10	1200.9	STRE C-N BEND C-H BEND N-H	1055.4	STRE C-N BEND C-H BEND N-H
11	1069.9	STRE C-N (square part) BEND C-H	933.1	STRE C-C (square part) Wagging N-H
12	989.5	STRE C-C TORS CH_3	686.4	OUT C-H (aro.)
13	682.5	OUT N-H	555.6	STRE C-S
14	554.9	STRE S-C	458.0	OUT O-H
15	349.5	Wagging O-H		

STRE; bond stretching, BEND; valence angle bending, OUT; out-of-plane bending and Wagging; valence angle bending between the planes.

3.3. NMR spectral analysis

Nuclear magnetic resonance (NMR) spectroscopy is one of the most frequently used methods in structure illumination. The chemical shift values for the ^{13}C and ^{1}H-NMR of the investigated compounds are given in Tables 3 and 4. Experimental ^{13}C and ^{1}H-NMR spectra of t' compounds were obtained in the DMSO-d_6+Na 18 in the D2O solvent [31]. Theoretical NMR spectra were calculated in the gas phase. Theoretical 13C and 1H NMR chemical shifts are presented in Tables 3 and 4 with reference to TMSO using the GIAO method [32] in the gas phase for the optimized structures obtained at the B3LYP/6-31G(d) level. The atomic labeling of the mentioned compounds for NMR data is indicated in Figure 3. The results of Table 3 and 4 show that the theoretical chemical shifts obtained by the DFT method are in good agreement with experimental data. The chemical shift values, which are slightly different from the experimental value, arising from the theoretical calculations taking place in isolated gas phase.

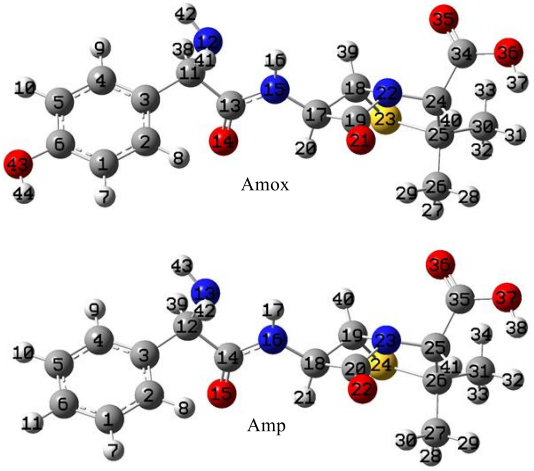

Figure 3. Labeling atomic number of Amox and Amp.

According to Table 3, 13C-NMR the chemical shift value of 6C for the Amox compound is greater than the chemical shift value of other carbons in the ring. Likewise, the chemical shift values of 13C, 19C and 34C for the compound are higher than the chemical shift values of the other carbons. This is a theoretically expected situation. Because the electronegative oxygen atom attracts more electrons from the carbon atoms it is bound to. In this case, the nuclei of these carbon atoms show less shielding effect. Less shielded nuclei show the higher chemical shift. The similar situation is valid for Amp compound in Table 3 and the hydrogen atoms in Table 4.

Computational studies have many advantages. Experimental NMR does not give the chemical shift value separately for atoms and the atoms with similar chemical structure entities have similar values. However, theoretical calculations give the value of individual chemical shifts for each atom and also illuminate many chemical shift values that are not observed experimentally.

Table 3. ^{13}C-NMR data of Amox and Amp

	Amox			Amp	
Atoms	Calc.	Exp.	Atoms	Calc.	Exp.
1C	107.9	115.0	1C	122.7	127.0
2C	122.3	131.4	2C	120.6	128.5
3C	128.1	128.1	3C	136.8	127.0
4C	124.5	131.4	4C	122.3	128.5
5C	108.5	115.0	5C	121.6	127.0
6C	147.5	156.8	6C	120.6	127.5
11C	61.1	57.2	12C	61.8	57.0
13C	159.4	173.1	14C	159.3	174.0
17C	67.3	57.5	18C	67.3	57.7
18C	76.6	67.0	19C	76.6	67.1
19C	161.3	170.0	20C	161.4	171.0
24C	68.8	73.9	25C	68.8	74.0
25C	70.1	64.6	26C	70.3	65.0
26C	34.5	31.8	27C	34.4	31.0
30C	25.7	27.5	31C	25.6	27.5
34C	156.1	173.6	35C	156.2	174.2

Table 4. ^{1}H-NMR data of Amox and Amp

	Amox			Amp	
Atoms	Calc.	Exp.	Atoms	Calc.	Exp.
7H	6.11	6.75	7H	7.23	7.45-7.31
8H	6.90	7.22	8H	7.04	7.45-7.31
9H	6.85	8.50	9H	6.90	7.45-7.31
10H	6.61	8.50	10H	7.16	7.45-7.31
16H	7.83	n.o.	11H	7.16	7.45-7.31
20H	5.37	5.45	17H	7.79	7.56
27H	1.59	1.49	21H	5.40	5.42
28H	1.23	1.49	28H	1.60	1.50
29H	1.65	1.49	29H	1.23	1.50
31H	1.15	1.59	30H	1.66	1.50
32H	1.64	1.59	32H	1.16	1.56
33H	1.66	1. 59	33H	1.64	1.56
37H	5.30	-	34H	1.67	1.56
38H	3.95	4.53	38H	5.31	-
39H	5.23	5.41	39H	3.93	4.54

40H	3.71	3.98	40H	5.25	5.46
41H	0.32	-	41H	3.71	3.97
42H	1.22	-	42H	0.40	n.o.
44H	3.48	n.o.	43H	1.27	n.o.

n.o. not observed.

3.4. Quantum chemical parameters

The molecular descriptors were calculated by using B3LYP/6-31G(d) level for investigation of inhibition efficiencies of β-lactam inhibitors given in Figure 1. The calculated molecular descriptors were given in Table 5 at gas phase. Abdallah experimentally identified the biological activities of these compounds and found that the inhibitory activity of Amox was greater than Amp [33].

Table 5. Quantum chemical parameters with B3LYP/6-31G(d) level in gas phase of inhibitors

Parameters	Amox	Amp
E_{HOMO}*	-5.962	-6.271
E_{LUMO}*	-0.414	-0.414
ΔE	5.549	5.857
η	2.774	2.928
σ	0.360	0.341
χ	3.188	3.343
μ	-3.188	-3.343
ω	1.832	1.908
ε	-8.845	-9.789

*E_{HOMO} and E_{LUMO} are given in eV unit

E_{HOMO} is a parameter associated with the electron donating ability of molecule [34,35]. If the E_{HOMO} increases, electron transfer tendency will increase to the LUMO of appropriate receptor molecules. The molecule having the higher E_{HOMO} indicates the higher inhibition effect. The order of the calculated E_{HOMO} values for these compounds is:

Amox >Amp

E_{LUMO} is a measure of electron accepting ability of chemical species. E_{LUMO} determines the polarizability of the compound i.e. the ability to be distorted by an electric field, and hence LUMO level receives electrons. Experimental and theoretical studies related to biological activity show that increasing of E_{LUMO} decreases the corrosion activities of molecules. Exchange of the calculated E_{LUMO} values for these compounds is:

Amox = Amp

The separation energy, ΔE is an important parameter as a function of reactivity of the molecule and chemical hardness is defined as resistance to electron transfer. The larger values of the HOMO-LUMO energy gap and chemical hardness will provide low reactivity for chemical species. The inhibition efficiencies orders according to ΔE gap and η will be similar to each other. The rankings of the ΔE and η values are:

Amox <Amp

Softness is the inverse of chemical hardness and represents high reactivity. Therefore, soft molecules exhibit high electron donating tendency and high biological activity effect. Exchange of the calculated σ values for these compounds is:

Amox >Amp

Absolute electronegativity is taken into account as a chemical descriptor in comparison of inhibition effects of chemical species. It should be noted that strong inhibitors should have low electronegativity values. Because inhibitors with low electronegativity are tended to give the electron. For a reaction of two systems with different electronegativity the electronic flow will occur from the molecule with the lower electronegativity towards that of higher value until the chemical potentials are equal [36,37]. The ranking of χ values for these compounds is:

Amox <Amp

Chemical potential is the inverse of the electronegativity. Therefore, the inhibition efficiency increases with increasing of chemical potential. Chemical hardness and softness, chemical potential are known as global reactivity descriptors [38]. According to the chemical potential, the inhibitor efficiency ranking should be:

Amox >Amp

Recently, Parr et al. have defined a new descriptor [39]. This parameter is a numeric expression of the global electrophilic power of the molecule that known as electrophilicity index (ω).

The electrophilicity index is a descriptor that represents the reactivity of the chemical species. The global electrophilicity index of the molecule allows quantitative classification of its reactive [40-44]. The electrophilicity index shows the ability of the electron-accepting ability [45]. According to the electrophilicity index, the inhibitor efficiency ranking should be:

Amox <Amp

Nucleophilicity index indicates the electron-donating ability of inhibitor molecules. The inhibition efficiency increases with increasing the ε value or decreasing the ω value. According to the nucleophilicity index, the inhibitor efficiency ranking should be:

Amox >Amp

If inhibitory activities in terms of the molecular properties of the β-lactam compounds are examined, this inhibitory efficiency rankings are an expected result. Amox among the first group of inhibitors are expected the condition to have higher inhibitory efficiency. The phenyl ring has a negative inductive effect. Moreover, OH group on the phenyl ring at Amox provides form stable complexes of compounds because it increases the electron density in the ring. Thus, localization of the electron pairs on the nitrogen atom of the NH_2 group increases. In this case, inhibitory efficiency increases of these molecules.

3.5. Molecular Electrostatic Potential (MEP) Maps

Molecular electrostatic potential (MEP) maps are used to predict the atom with the higher electron density in a molecule. MEP is the potential generated by the charge distribution of a molecule and denotes chemical reactivity, showing nucleophilic and electrophilic sites indicated by MEP contour maps [46]. For the consideration of the reactive behavior of a chemical system and to investigate the molecular structure with its physiochemical property relationships, the three-dimensional distribution of its MEP is helpful [47]. In MEP diagram negative regions can be regarded as nucleophilic centers [48]. Negative electrostatic potential corresponds to the attraction of a proton by the concentrated electron density in the molecule (lone pairs, pi-bonds); thus, revealing sites for electrophilic attack (colored in shades of red in standard contour diagrams) Positive electrostatic potential corresponds to the repulsion of a proton by the atomic nuclei in regions where low electron density exists and the nuclear charge is incompletely shielded (colored in shades of blue in standard contour diagrams) [49]. Theoretical methods can be used to answer these questions that may be greatly helpful in designing other and better drugs. Molecular electrostatic potentials (MEP) computed using ab initio methods can be particularly useful in this context since MEP is known to be a reliable descriptor of hydrogen bonding [50–55].

The MEP maps of inhibitors which calculated B3LYP/6-31G(d) are given in Figure 4. The third region with higher electron density is labeled in maps. These regions are referred to as Zone 1, Zone 2 and Zone 3. According to this diagram will be protonated regions. Zone 1,2 and 3 have protonated region for Amox (14, 21 and 35O), Amp (15, 22 and 36O). As a result, the MEP map show that the negative potential region is on oxygen atom which is the biologically active region.

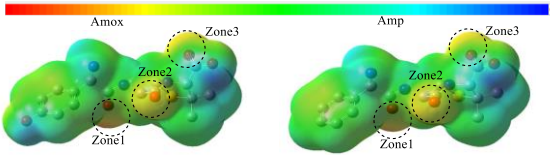

Figure 4. The MEP maps of the neutral inhibitor molecules at HF/6-31++G(d,p) level in gas phase

3.6. Non-Linear Optical (NLO) Properties

NLO is important property in providing the key functions of frequency shifting, optical modulation, optical switching, optical logic and optical memory for the technologies in areas such as telecommunications, signal processing and optical interactions [10]. In the recent studies, NLO is attracted a lot of attention. Organic molecules exhibit significantly NLO properties due to delocalized π electron moving along the molecule. NLO materials are categorized as semiconductor multilayer structures. Therefore, a wide variety of molecular systems inorganic, organic and organometallic were investigated for NLO activity. Some quantum chemical descriptors which are total static dipole moment (μ), the average linear polarizability (α), the anisotropy of the polarizability (Δα) and first hyperpolarizability (β)

have been used for explaining the NLO properties in many computational studies. NLO properties and urea is taken according to standards were calculated at the DFT/B3LYP/6-31G(d) level for the studied ligand. These parameters are given in Table 6.

Table 6 The calculated dipole moment (μ), average linear polarizability (α), the anisotropy of the polarizability (Δα) and hyperpolarizability (β) for urea and investigated molecules.

	μ(D)	α/(Å^3)	Δα/(Å^3)	β_0 (cm^5/esu)x10^{-30}
Urea	1.8059	2.0958	8.8780	297.3869
Amox	1.1490	23.4659	58.9546	2539.9904
Amp	0.5947	25.4659	66.6607	938.9493

NLO properties can be affected from polarizability, the anisotropy of the polarizability and hyperpolarizability. NLO properties increase with increasing the linear polarizability, the anisotropy of the polarizability and first hyperpolarizability. According to Table 3, all values of each mentioned molecules are greater than their urea values. Therefore, NLO properties of Amox and Amp are better than urea and these molecules can be used as NLO material [56].

3.7. Molecular Docking Study

Molecular docking is an effective tool used to achieve binding affinity between the identified ligand and the appropriate target protein of this ligand. Docking is a program that is allowed to interact with a chemical known as a 'receptor' and a chemical entity known as a 'ligand' in a software to analyze interactions between the receptor and ligand. The interaction can be analyzed by evaluating various parameters such as the free energy of binding (kcal/mol). Binding energy is a measure of the affinity of the ligand-protein complex [57]. As the energy decreases, the stability of the complex increases. Computational approaches can be a method for filtering molecules before the experimental test. Docking methods may need a combination with other computational methods for structure-activity relationships [58].

The starting structure was selected by PDB Database (PDB ID: 1NRL) for Amox and Amp and the molecular docking calculations were performed on AutoDock [59] is a free open source software package for virtual placement of small molecules into macromolecular receptors and developed for making related accounts. For this reason, all ligands were studied in the docking program with this target protein. The interaction between the ligands and the target enzyme are presented in the Figure 5.

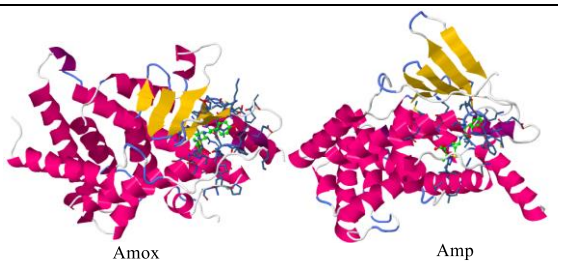

Figure 5. Ligands (green balls) interaction with protein 2J9N.

According to molecular docking result, interaction energies that occur when ligands bind to the protein for Amox and Amp is -9.0 and -8.29 kcal/mol, respectively. These results show that the inhibition efficiency of Amox is higher than Amp. Ki provides information that predicts that a ligand can inhibit an enzyme and interact with a substrate for the enzyme. Docking server inhibition constant for Amox and Amp is 229.81 and 837.77 nM, respectively. If Ki is smaller, less drug is needed to inhibit the enzyme activity and this situation shows that the ligands are within reasonable limits [60]. If vdW is hydrogen bond and dissolved energy is negative, the ligand is well attached to an active site on the target molecule. Similarly, if the electrostatic energy is negative, this negative value proves that the ligands are linked to the target molecule [61]. These values in the molecular docking results are negative for the ligands. So, it can say it is appropriate for the selected target molecule ligands. In accordance with the docking server which gives the binding site analysis, the ligands interacted well with the protein in the docking grid.

The hydrogen bond between Amox and 1NRL is between the nitrogen atoms of the ligand and LEU209 and SER238 of the target proteins. Polar bonds are between the hydrogen atom of the ligand SER238. There are hydrophobic bonds between the carbon atoms in the ligand and LEU206, LEU209, PRO227, LEU239, MET243, HIS407 and ILE414.

The hydrogen bonds for Amp are between nitrogen atoms LEU209. Polar bonds are between oxygen atoms and SER247. π-π interactions occur between the carbon atoms of the ligand and HIS407. The hydrophobic interactions of this ligand exist between the carbon atoms and LEU239, LEU240, MET243 and LEU411. According to molecular docking calculations, the most important interaction is the hydrogen bond interaction. Amox has made more H-bonds than Amp. As a result, according to experimental, theoretical and docking studies, Amox is a molecule with a higher inhibitory activity than Amp.

4. Conclusion

Amoxicillin (Amox) and ampicillin (Amp) were calculated at B3LYP/6-31G(d) level. The optimized geometrical parameters are in good agreement with crystal data. The theoretical and experimental results for some strecthing frequencies are very close to each other. It was observed that the theoretical chemical shifts obtained by the DFT method were in good agreement with the experimental data and it was thought that the difference between the experimental values and the calculated chemical shift values was derived from the theoretical calculations in the isolated gas phase. The biological activity suggested from the quantum chemical parameters and the experimental induction activities gave very similar results for the molecules. MEP maps for Amox and Amp show that the biologically active region is on the oxygen atom. NLO properties of Amox and Amp are better than urea and these molecules can be used as NLO material. As a result, according to experimental, theoretical and docking studies, Amox is a molecule with a higher inhibitory activity than Amp.

Acknowledgment

This research was made possible by TUBITAK ULAKBIM, High Performance and Grid Computing Center (TR-Grid e-Infrastructure).

References

[1] John D. Buynak. Understanding the longevity of the b-lactam antibiotics and of antibiotic/b-lactamase inhibitor combinations. Biochemical pharmacology, 71(2006)930 – 940.

[2] Gökhan Gece, Drugs: A review of promising novel corrosion inhibitors, Corrosion Science, 53 (2011) 3873–3898

[3] M.S. Forman, J.Q. Trojanowski, V.M-Y. Lee, Neurodegenerative diseases: a decade of discoveries paves the way for therapeutic breakthroughs, Nat. Med., 10 (2004) 1055–1063.

[4] J.D. Rothstein, S. Patel, M.R. Regan, C. Haenggeli, Y.H. Huang, D.E. Bergles, L. Jin, M.D. Hoberg, S. Vidensky, D.S. Chung, S.V. Toan, L.I. Bruijn, Z.Z. Su, P. Gupta, P.B. Fisher, b-Lactam antibiotics offer neuroprotection by increasing glutamate transporter expression, Nature, 433 (2005) 73–77.

[5] K.J. Barnham, C.L. Masters, A.I. Bush, Neurodegenerative diseases and oxidative stress, Nat. Rev. Drug Discov., 3 (2004) 205–214.

[6] J.S. Valentine, P.J. Hart, Bioinorganic chemistry special feature: misfolded CuZnSOD and amyotrophic lateral sclerosis, Proc. Natl. Acad. Sci. USA, 100 (2003) 3617–3622.

[7] M. Azzouz, P. Poindron, S. Guettier, N. Leclerc, C. Andres, J.M. Warter, J. Borg, Prevention of mutant SOD1 motoneuron degeneration by copper chelators in vitro, J. Neurobiol., 42 (2000) 49–55.

[8] A. Sher, M. Veber, M. Marolt-Gomisˇcˇek, Spectroscopic and polarographic investigations: copper (II)–penicillin derivatives, Int. J. Pharm., 148 (1997) 191–199.

[9] A. Sher, M. Veber, M. Marolt-Gomiscek, S. Gomiscek, The study of complexation of copper(II) with ampicillin. I. Spectroscopic and electrochemical investigations of interactions at equilibrium conditions, Int. J. Pharm., 90 (1993) 181–186.

[10] G. Mukherjee, T. Ghosh, Metal ion interaction with Penicillins. Part VII: Mixed-ligand complex formation of cobalt(II), nickel(II), copper(II), and Zinc(II) with ampicillin and nucleic bases, J. Inorg. Biochem. 59 (1995) 827–833.

[11] Valentina Gamba, Guglielmo Dusi, Liquid chromatography with fluorescence detection of amoxicillin and ampicillin in feeds using pre-column derivatization, Analytica Chimica Acta, 483 (2003) 69–72.

[12] Şirin Bitmez, Koray Sayin, Bariş Avar, Muhammet Köse, Ahmet Kayraldız, Mükerrem Kurtoğlu, Preparation, spectral, X-ray powder diffraction and computational studies and genotoxic properties of new azo–azomethine metal chelates, 1076 (2014) 213–226.

[13] P. Politzer, D.G. Truhlar, Chemical Applications of Atomic and Molecular Electrostatic Potentials. Academic Press, New York, 1981.

[14] A. Bergamo, G. Sava, Dalton Trans., 40 (2011) 7817-7823.

[15] C. G. Hartinger, M. A. Jakupec, S. Zorbas-Seifried, M. Groessl, A. Egger, W. Berger, H. Zorbas, P. J. Dyson, B. K. Keppler, Chem. Biodiversity, 5 (2005) 2140-2154.

[16] Mohamed K. Awad, Mohamed R. Mustafa, Mohamed M. Abo Elnga, Computational simulation of the molecular structure of some triazoles as inhibitors for the corrosion of metal surface, Journal of Molecular Structure: THEOCHEM, 959 (2010) 66–74.

[17] Jeffrey P. Merrick, Damian Moran, Leo Radom, An Evaluation of Harmonic Vibrational Frequency Scale Factors, J. Phys. Chem., A 2007, 111, 11683-11700.

[18] D. Sajan, J. Hubert, V.S. Jayakumar, J. Zaleski, J. Mol. Struct., 785 (2006) 43–53.

[19] T. Koopmans, Physica, 1 (1933) 104

[20] S. Kaya, S. Erkan Kariper, A. Ungördü, C. Kaya, Effect of Some Electron Donor and Electron Acceptor Groups on Stability of Complexes According to the Principle of HSAB, Journal of New Results in Science, 4 (2014) 82-89.

[21] D.B. Alexander, A.A. Moccari, Evaluation of corrosion inhibitors for component cooling water systems, Corrosion Science., 49 (1993) 921–928.

[22] V.S. Sastri, J.R. Perumareddi, Corrosion, 53 (1996) 671.

[23] W. Kohn, L.J. Sham, Quantum density oscillations in an inhomogeneous electron gas, Physical Review, 137 (1965) A1697–A1705.

[24] R.G. Pearson, Inorg. Chem., 27 (1988) 734.

[25] R. G. Parr, V.Szentpaly, S. Liu, J.Amc. Chem. Soc., 121(1999) 1922

[26] S. Kiyooka, D. Kaneno, R. Fujiyama, Tetrahedron Letters, 54 (2013) 339.

[27] Koray Sayin, Duran Karakas, Nihat Karakus, Tuba Alagöz Sayin, Zinet Zaim, Sultan Erkan Kariper, Spectroscopic investigation, FMOs and NLO analyses of Zn(II) and Ni(II) phenanthroline complexes: A DFT approach, Polyhedron, 90 (2015) 139–146.

[28] http://cccbdb.nist.gov/vibscalejust.asp

[29] D. Rajaraman, G. Sundararajan, N.K. Loganath, K. Krishnasam, Synthesis, molecular structure, DFT studies and antimicrobial activities of some novel 3-(1-(3,4-dimethoxyphenethyl)-4,5-diphenyl-1H-imidazol-2-yl)-1H-indole derivatives and its molecular docking studies, Journal of Molecular Structure, 1127 (2017) 597-610.

[30] R. Di Stefano, M. Scopelliti, C. Pellerito, T. Fiore, R. Vitturi, M.S. Colomba, P. Gianguzza, G.C. Stocco, M. Consiglio, L. Pellerito, Organometallic complexes with biological molecules XVII. Triorganotin(IV) complexes with amoxicillin and ampicillin, Journal of Inorganic Biochemistry, 89 (2002) 279–292.

[31] R. Ditchfield, Molecular orbital theory of magnetic shielding and magnetic susceptibility, J. Chem. Phys., 56 (1972) 5688-5692.

[32] M. Abdallah, Antibacterial drugs as corrosion inhibitors for corrosion of aluminium in hydrochloric solution. Corrosion Science, 46 (2004) 1981–1996.

[33] D.B. Alexander, A.A. Moccari, Evaluation of corrosion inhibitors for component cooling water systems, Corrosion, 49 (1993) 921–928.

[34] A.J. LopesJesus, Luciana I.N. Tomé, M. Ermelinda, S. Eusébio, Mário T.S. Rosado, J.S. Redinha, Hydration of cyclohexylamines: CPCM calculation of hydration gibbs energy of the conformers, Journal of Physical Chemistry A, 111 (2007) 3432–3437.

[35] P. Udhayakala, A. Maxwell Samuel, T. V. Rajendiran and S. Gunasekaran, Quantum chemical study on inhibitory action of some

substituted 1,3,4-oxadiazoles on mild steel, Der Pharmacia Lettre, 5 (2013) 272-283.

[36] Martınez S, Mater Chem and Phys., 77(2002) 97-102.

[37] R. Parthasarathi, V. Subramanian, D. R. Roy and P. K. Chattaraj, Electrophilicity index as a possible descriptor of biological activity, Bioorganic & MedicinalChemistry, 12 (2004) 5533–5543.

[38] R. G. Parr, V.Szentpaly, S. Liu, J.Amc. Chem. Soc., 121 (1999) 1922.

[39] Parthasarathi, R.; Padmanabhan, J.; Subramanian, V.; Maiti, B.; Chattaraj, P. K. J. Phys. Chem. A, 107 (2003) 10346.

[40] Thanikaivelan, P.; Subramanian, V.; Raghava Rao, J.; Nair, B. U. Chem. Phys. Lett., 323 (2000) 59.

[41] Parthasarathi, R.; Padmanabhan, J.; Elango, M.; Subramanian, V.; Chattaraj, P. K. Chem. Phys. Lett., 394 (2004) 225.

[42] Parthasarathi, R.; Padmanabhan, J.; Subramanian, V.; Maiti, B.; Chattaraj, P. K. Curr. Sci., 86 (2004) 535.

[43] Parthasarathi, R.; Padmanabhan, J.; Subramanian, V.; Sarkar, U.; Maiti, B.; Chattaraj, P. K. Internet Electron J. Mol. Des., 2 (2003) 798.

[44] N.O. Obi-Egbedi, I.B. Obot, M.I. El-Khaiary, Quantum chemical investigation and statistical analysis of the relationship between corrosion inhibition efficiency and molecular structure of xanthene and its derivatives on mild steel in sulphuric acid, Journal of Molecular Structure, 1002 (2011) 86-96.

[45] P. Politzer, D.G. Truhlar, Chemical Applications of Atomic and Molecular Electrostatic Potentials. Academic Press, New York, 1981.

[46] M. Wagener, J. Sadowysky, J. Gasteiger, J. Am. Chem. Soc., 117 (1995) 7769–7775.

[47] Jayaraman Jayabharathi, Venugopal Thanikachalam, Marimuthu Venkatesh Perumal, Natesan Srinivasan, Fluorescence resonance energy transfer from a bio-active imidazole derivative 2-(1-phenyl-1H-imidazo[4,5-f][1,10]phenanthrolin-2-yl)phenol to a bioactive indoloquinolizine system, Spectrochimica Acta Part A, 79 (2011) 236–244.

[48] G.C. Muscia, Synthesis trypanocidal activity and molecular modeling studiesof 2-alkylaminomethylquinoline derivatives, European Journal of Medicinal Chemistry, 46 (2011) 3696-3703.

[49] P.S. Kushwaha, P.C. Mishra, Int. J. Quant. Chem., 76 (2000) 700.

[50] A. Kumar, C.G. Mohan, P.C. Mishra, J. Mol. Struct. (Theochem), 361 (1996) 135.

[51] C. Santosh, P.C. Mishra, J. Mol. Model, 3 (1997) 172.

[52] P.C. Mishra, A. Kumar, J.S. Murray, K.D. Sen (Eds.), Molecular Electrostatic Potentials: Concepts and Applications, Theoretical and Computational Chemistry Book Series, Elsevier, Amsterdam, 3 (1996) 257.

[53] A.K. Singh, P.S. Kushwaha, P.C. Mishra, Int. J. Quant. Chem., 82 (2001) 299.

[54] M.K. Shukla, P.C. Mishra, J. Mol. Struct. (Theochem), 340 (1995) 159.

[55] Muhammet Kose, Ceylan Hepokur, Duran Karakas, Vickie McKee, Mukerrem Kurtoglu, Structural, computational and cytotoxic studies of square planar copper(II) complexes derived from dicyandiamide, Polyhedron, 117 (2016) 652–660.

[56] Ramchander Merugu, Uttam Kumar Neerudu, Karunakar Dasa, Kalpana V. Singh, Molecular docking studies of deacetylbisacodyl with intestinal sucrase-maltase enzyme, International Journal of Advances in Scientific Research, 2 (2016) 191-193.

[57] Sugio S, Kashima A, Mochizuki S, Noda M, Kobayashi K. Crystal structure of human serum albumin at 2.5 Aresolution. Protein Eng.,12 (1999) 439-46.

[58] Khandelwal A, Krasowski MD, Reschly EJ, Sinz M, Swaan PW and Ekins S Machine learning methods and docking for predicting human pregnane X receptor activation. Chem Res Toxicol, (2008).

[59] Ramchander Merugu, Uttam Kumar Neerudu, Karunakar Dasa, Kalpana V. Singh, Molecular docking studies of deacetylbisacodyl with intestinal sucrase-maltase enzyme, International Journal of Advances in Scientific Research, 2 (2016) 191-193.

[60] Dipita Bhakta, Ramamoorthy Siva, Morindone, an Anthraquinone, Intercalates DNA Sans Toxicity: a Spectroscopic and Molecular Modeling Perspective, Appl Biochem Biotechnol 167 (2012) 885–896.